



ECM-based macroporous sponges release essential factors to support the growth of hematopoietic cells

Neta Soffer-Tsur^{a,b}, Dan Peer^{b,c,d}, Tal Dvir^{a,c,d,*}

^a Laboratory for Tissue Engineering and Regenerative Medicine, Tel Aviv 69978, Israel

^b Laboratory for Precision NanoMedicine, School for Molecular Cell Biology and Biotechnology, Tel Aviv 69978, Israel

^c Department of Materials Science and Engineering, Tel Aviv 69978, Israel

^d Center for Nanoscience and Nanotechnology, Tel Aviv University, Tel Aviv 69978, Israel

ARTICLE INFO

Article history:

Received 25 August 2016

Accepted 20 September 2016

Available online 23 September 2016

Keywords:

Tissue engineering

Scaffolds

Hematopoietic cells

ABSTRACT

The success of hematopoietic stem cells (HSCs) transplantation is limited due to the low number of HSCs received from donors. *In vivo*, HSCs reside within a specialized niche inside the 3D porous spongy bone. The natural environment in the niche is composed of structural proteins, glycosaminoglycans (GAGs) and soluble factors that control cells fate. However, the designed scaffolds for *in vitro* culture do not fairly recapitulate this microenvironment and cannot efficiently control HSCs fate. Here we report on the development of new omental ECM-based 3D macroporous sponges for hematopoietic cell culture. The scaffolds' structure, porosity and stability were characterized and optimized. Analysis of the biochemical content revealed that they were composed of collagens and GAGs, including sulfated GAGs. This morphology and composition enabled growth factors interaction with the sulfated GAGs, as indicated by the high loading capacity and release profile of three different hematopoietic niche factors. Finally, the ability of the ECM-based scaffolds to efficiently support the growth of hematopoietic cells by releasing stem cell factor (SCF) was demonstrated.

© 2016 Elsevier B.V. All rights reserved.

1. Introduction

Transplantation of hematopoietic stem cells (HSCs) has the potential of treating hematologic disorders such as different types of leukemia, immune deficiencies and autoimmune diseases. Unfortunately, the success of HSCs transplantation is limited due to the low number of HSCs received from the donor. This results in a significant delay in hematopoiesis, accounting for the relatively high transplant-related mortality rate [1]. Successful HSC expansion studies have spanned over the last three decades. However a routine method for efficient *ex-vivo* expansion of HSCs is still an unmet need [2].

In vivo, HSCs reside within a specialized niche inside the spongy bone. In this 3D porous structure, glycosaminoglycans (GAGs) and proteins, including collagen type I, fibronectin and laminin, provide physical support and topographical cues to the HSCs [3]. Soluble factors, such as stem cell factor (SCF), Fms-related tyrosine kinase 3 ligand (Flt3L) and vascular endothelial growth factor (VEGF) electrostatically interact with sulfated GAGs, which act as a protein depot. According to the physiological need these growth factors are released to initiate signaling pathways determining cell fate [3–6].

One of the goals in tissue engineering is to design 3D biomaterials that closely mimic the natural ECM, in order to properly maintain cell growth [7–9]. However, the detailed biochemical composition of the natural matrix, which best foster cellular organization is still not completely understood. Therefore, synthetic recapitulation of this microenvironment is a complicated task [8,10,11]. Consequently, decellularized matrices were developed and used in order to supply the cells with the essential biochemical cues that efficiently support their growth. During decellularization process, cells are gently removed from a harvested tissue or organ by chemical, physical and biological methods [8], while the essential biomolecules are preserved [12]. Recent works have demonstrated the engineering of functional cardiac, hepatic and lung tissues by using different decellularized matrices from the heart, liver and the omentum [13–17].

The omentum is a highly vascularized adipose tissue that extends from the stomach overlying the abdomen [18]. Its ECM is rich with different types of collagens, hyaluronan, sulfated GAGs and growth factors [19,20], making it an ideal microenvironment for stem cells, with proven regenerative capabilities [21,22]. In a recent work our group has demonstrated the potential of omentum-based scaffolds or hydrogels to engineer cardiac tissues [22–24]. We have further optimized the decellularization process of the tissue in order to obtain a better balance between complete decellularization and preservation of essential ECM components such as GAGs [23,24]. Here we report on the development

* Corresponding author.

E-mail address: tdvir@post.tau.ac.il (T. Dvir).

of new omental ECM-based 3D macroporous sponges. The new cell-supporting scaffolds are based on the ability to liquefy the decellularized omentum [25], casting and lyophilizing to create homogenous and porous microenvironment. We have investigated the physical and biochemical properties of the obtained scaffolds and assessed the potential of the preserved sulfated GAGs (s-GAGs) to serve as a depot for essential growth factors related to the bone marrow niche. We have further demonstrated the potential of the scaffolds to slowly release the factors into the cellular microenvironment, serving as an effective platform for hematopoietic cell growth.

2. Materials and methods

All materials were purchased from Sigma (Rehovot, Israel) unless stated otherwise.

2.1. Decellularization

Omenta of healthy pigs were purchased from the institute of animal research in Kibutz Lahav, Israel. All steps of incubations and washes were obtained at room temperature on an orbital shaker unless noted otherwise.

Fresh omentum was washed with phosphate buffered saline (PBS) in order to deplete blood and debris. The tissue was then agitated in a hypotonic buffer of 10 mM Tris 5 mM Ethylenediaminetetraacetic acid (EDTA) and 1 μ M phenylmethanesulfonyl-fluoride (PMSF) at pH 8.0. Next, the tissue went through three cycles of freezing (-80°C) and thawing (37°C) using the same buffer. After the last thawing the tissue was dehydrated by 70% ethanol wash, followed by three 100% ethanol washes. Lipid extraction was then conducted by washing the omentum with 100% acetone following 24 h agitation in 60/40 (v/v) hexane:acetone solution. The defatted tissue was rehydrated, washed and incubated in 0.25% Trypsin-EDTA (Biological Industries, Kibbutz Beit-Haemek, Israel) solution overnight for cell removal. The tissue was then washed thoroughly with PBS. For nucleic acids elimination the tissue was then incubated in 1.5 M sodium chloride solution for 24 h. Next, the processed omentum was washed with 50 mM Tris 1% Triton-X100 solution at pH 8.0 for 1 h. Finally, the tissue was washed with PBS and with double distilled water before freezing and lyophilizing.

2.2. Gel formation

The lyophilized decellularized omentum was ground into powder using Wiley Mini-Mill. Different quantities of the powder were farther digested by 1 mg/ml pepsin solution in 0.1 M HCl, creating different concentrations (0.5%, 1% and 1.5% w/v). the digestion process was conducted in room temperature, using slow stirring. The digestion was terminated by pH adjustment to 7.2–7.4 using NaOH.

Measured volumes of solution were casted in round wells and incubated in 37°C for gelation.

2.3. Porous scaffolds formation

Three different freezing regimes were used in order to obtain different porosity. The gels were either frozen in liquid nitrogen, placed inside a -20°C freezer, or slowly frozen in an isopropanol bath inserted in -20°C freezer overnight. All frozen gels were lyophilized under the same conditions. The lyophilized scaffolds were incubated overnight in PBS at 37°C and then washed with double distilled water. The washed scaffolds were lyophilized again.

2.4. DNA staining and quantification

For nucleic acid detection, small pieces from the native and the processed tissues were stained with 5 $\mu\text{g}/\text{ml}$ Hoechst 33258 for 3 min,

followed by PBS washes. The samples were visualized using an inverted fluorescence microscope (Nikon Eclipse TI).

DNA was extracted from three scaffolds and three random 25–30 mg dried samples of the native tissue using a DNeasy Blood & Tissue Kit (Qiagen, Hilden, Germany) according to the manual guide. The obtained DNA was quantified by measurements of the O.D at 260 nm wavelength using spectrophotometer (Nanodrop 1000, Thermo Scientific).

2.5. Scanning electron microscopy

For scanning electron microscope (SEM) imaging, cross sections of the lyophilized scaffolds were sputter-coated with gold and then observed under SEM (Jeol JSM840A). The properties of the pores from three different scaffolds measured with ImageJ program (NIH).

2.6. Sulfated glycosaminoglycan quantification

The sulfated glycosaminoglycans (GAGs) in the native omentum and the processed scaffolds were quantified using the Blyscan™ sulfated GAG assay kit (Biocolor Ltd., Carrickfergus, UK) according to the manufacturer instructions. Briefly, the tissues were digested with papain. The digested solutions were centrifuged and the supernatants were examined with dimethylmethylene blue. Overall, three samples were picked for each assay.

2.7. Histology

Wet scaffolds were placed inside optimum cutting temperature (O.C.T.) embedding medium (Tissue-Tek, Sakura, Japan) and snap frozen in liquid nitrogen. Sections of 20 μm were obtained using a Cryotome™ FSE (Thermo scientific) and affixed to X-tra® adhesive glass slides (Leica Biosystems, Wetzlar, Germany). The slides were stained with Alcian-blue and Fast-red (Merck) for GAG imaging. Masson's trichrome (Bio-Optica, Milano, Italy) for cell and collagen detection staining were performed according to the manufacturer's guidelines.

2.8. Measurements of growth factors loading and release from the scaffolds

For the sustained release assay, triplicates of lyophilized scaffolds or empty wells were loaded in non-binding 96-well plates (Corning) with 50 ng of stem cell factor (SCF), FMS-like tyrosine kinase (Flt3-L) or vascular endothelial growth factor (VEGF) all purchased from PeproTech Asia. The loaded scaffolds were incubated for 2 h at 37°C , and then washed once with PBS-0.1% bovine serum albumin (BSA). The scaffolds were incubated in PBS-0.1% BSA at 37°C for 10 days. The medium was collected and replaced at different time points (1, 2, 4, 7 and 10 days) and preserved at -20°C for analysis.

The samples were thawed, diluted and examined by enzyme linked immune-sorbent assay (ELISA) for the different growth factors (ELISA kits for Flt3-L and SCF were purchased from PeproTech Asia, duo-set ELISA kit for VEGF was purchased from R&D Systems®).

For the loading assay, triplicates of lyophilized scaffolds were loaded with 50, 100, 200 or 400 ng of SCF, Flt3-L or VEGF. The loaded scaffolds were incubated for 2 h at 37°C and then washed once with PBS - 0.1% BSA. The scaffolds were digested using 2.5 mg/ml collagenase type I in PBS - 0.1% BSA solution at 37°C for 1 h. the digested samples were examined by ELISA for the different growth factors.

2.9. Erythroid myeloid lymphocyte (EML) cells growth within the scaffolds

EML cells were purchased from ATCC® and handled as instructed. Briefly, the cells were cultured in humidified incubator with 5% CO_2 at 37°C , in Iscove's modified Dulbecco's medium (IMDM, from ATCC®), containing 200 ng/ml mouse SCF (PeproTech Asia) and 20% heat-inactivated fetal bovine serum (Biological industries).

In order to determine the EML cells response to different SCF concentrations, $4 \cdot 10^5$ cells were placed in each well in 96-well plate with different SCF concentrations (0, 50, 100 or 200 ng/ml) in triplicates. The cells were incubated at 37 °C for 72 h, and then incubated with XTT reagents (Biological industries, Beit Haemek, Israel) for 2 h at 37 °C for evaluation of cell viability. The optical density of the medium was measured at 450 nm and 630 nm.

Triplicates of dry scaffolds of omentum or empty wells, as control (in a 96-well plate), were incubated with 5 μ l of medium supplemented with different concentrations of SCF (0, 50 or 200 ng/ml) for 1 h at 37 °C. Following, $4 \cdot 10^5$ EML cells in 5 μ l droplets were seeded in the scaffolds or on the wells without the scaffolds. Ninety milliliters of medium without SCF were added to each well. XTT viability assay was conducted at day 0 (2 h post seeding), and after 72 h. The proliferation was determined as the ratio between the XTT results of day 3 and day 0.

2.10. Statistical analysis

Statistical analysis data are presented as average \pm standard error. Differences between the groups were assessed with *t*-test. All analyses were performed using GraphPad Prism version 6.00 for Windows (GraphPad Software). $p < 0.05$ was considered significant. NS denotes that no significant difference was detected.

3. Results and discussion

In order to obtain an effective decellularized scaffold for tissue engineering, the balance between preservation of essential biomolecules and elimination of all cellular components must be achieved. We have recently demonstrated a comparison between five different omentum decellularization methods [23]. The effect of the different step during the process could be easily detected in a macroscopic view (Fig. 1A). The omentum was transformed from a pink fatty tissue to a completely white and highly hydrophilic substance. In order to obtain the liquid form of the omentum, the decellularized tissue was digested with pepsin, molded into appropriate wells and cross-linked in 37 °C. The cross-linked hydrogels were then frozen and lyophilized, achieving solid, stable and highly porous sponges that preserve their shape and size after rehydration (Fig. 1B).

When using decellularized matrices for culturing cells and eventually for transplantation, it is essential to remove all antigens from material to prevent an immune response or contamination [8,26]. Therefore, our next step was to verify a complete cell removal by Hoechst 33258

staining. As can be seen in Fig. 2A, while nuclei were clearly seen at the native tissue, they were not detected in the processed tissue (Fig. 2B). Further quantification of the residual DNA (Fig. 2C) revealed significant reduction in DNA due to the decellularization process, resulting in <50 ng DNA per mg dry scaffold (33.57 ± 9.41 ng DNA/mg scaffold). This value is considered as complete decellularized, which is sufficient to prevent an immune response [27].

We next sought to evaluate the biochemical composition of the scaffolds by histological staining. Masson trichrome staining revealed that the scaffolds are mainly composed of collagens (Fig. 2D). As this histological staining detects nuclei and cytoplasm as well, the lack of staining for these cellular components further supported our successful decellularization results. Alcian Blue - Fast Red staining detected the presence of glycosaminoglycans (GAGs) in the pore walls (Fig. 2E). Preservation of these molecules during the decellularization process is extremely important. When the GAGs are sulfated (s-GAGs), their negatively charged sulfate groups can electrostatically interact with growth factors and cytokines. *In vivo*, within the bone marrow or in other tissues this interaction is exploited to retain the factors and slowly release them into the cellular microenvironment according to the demand of the cells [28,29]. Therefore, we next sought to assess the concentration of s-GAGs in the scaffolds compared to the native omentum by a Blyscan™ sulfated GAGs assay kit. The native omentum contained 0.60 ± 0.007 μ g sulfated GAGs per mg tissue, whereas the scaffolds contained 1.36 ± 0.033 μ g s-GAGs per mg scaffold (Fig. 2F). The content of the sulfated GAGs in the processed omentum was significantly higher than in the native, due to the decellularization and fat extraction processes, which increased and packed the concentration of the a-cellular components of the tissue. The preservation of the sulfated GAGs within the scaffolds indicates that they can be utilized to control the release of positively-charged biofactors during cell culture period. Controlled exposure of the cultured cells to the growth factors may affect physiological processes, such as cell proliferation, differentiation, and migration.

Another parameter that controls cell fate is the porous structure of the scaffold. The pores need to be large enough to enable cells proliferation and migration for formation of new tissues. On the other hand, the pores should be small enough to enable sufficient contact between the cells and the surface, facilitating extracellular signaling and delivery of nutrients [30,31]. In order to obtain the optimal topography, the porosity of the scaffold can be controlled by changing the physical conditions during the biofabrication process. Prior to the lyophilization process the hydrogel is frozen to create water crystals, which are later on removed

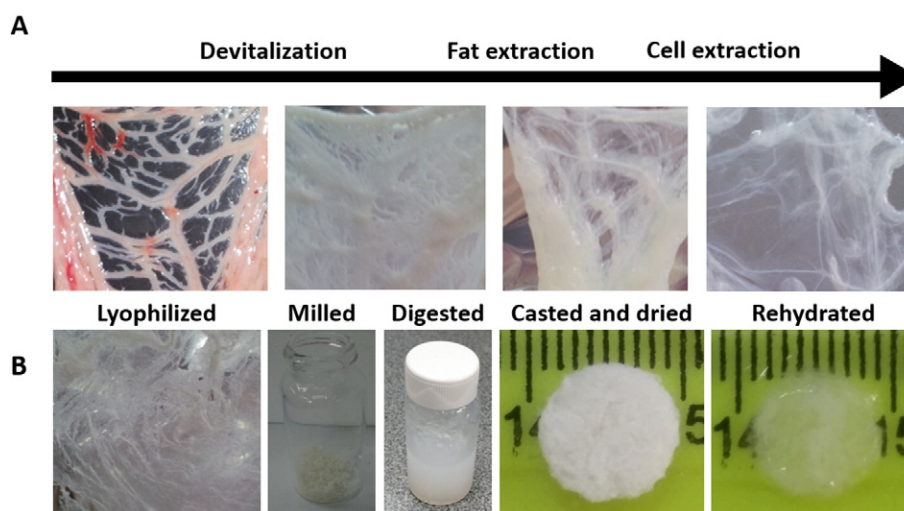


Fig. 1. Scaffold fabrication process. A. Macroscopic view on the different stages of the omentum decellularization method. First the tissue is devitalized by freezing and thawing in hypotonic buffer. Following, the lipids are extracted using organic solvents. Finally, cellular components are removed by trypsin, NaCl and triton. B. Scaffolds formation: the lyophilized decellularized omentum is grounded into powder, digested with pepsin, cross-linked to the desired shape and lyophilized, to create a stable sponge.

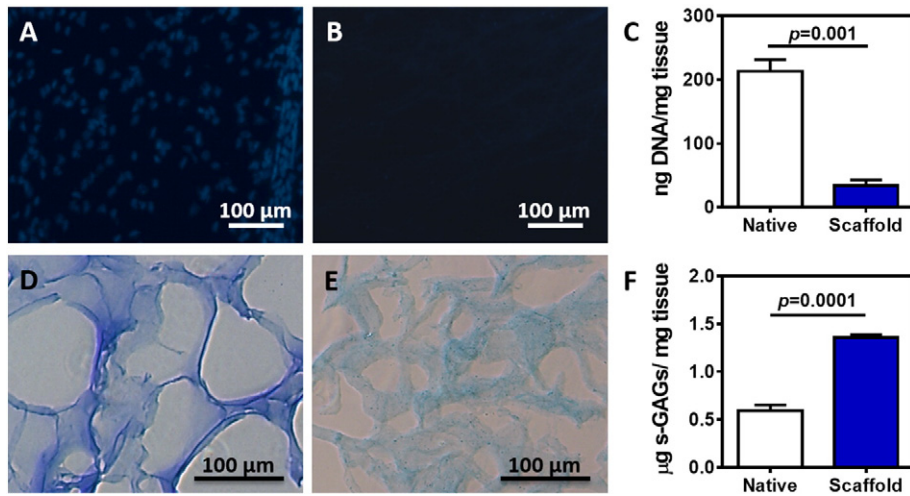


Fig. 2. Biochemical components of the decellularized omentum. A. Hoechst staining of the native omentum. B. Hoechst staining of the decellularized tissue. C. DNA quantification in ng per mg tissue of the native omentum and the decellularized scaffold ($n = 3$). D. Masson's trichrome staining of frozen sections of the scaffold. Collagen fibers are stained blue. Nuclei and cytoplasm could not be detected. E. Alcian blue and fast red staining of frozen cuts of the scaffold. GAGs are stained in light blue. F. Quantification of sulfated GAGs in the native omentum and within the decellularized scaffolds. Results are presented as mean µg sulfated GAGs per mg dry mass ($n \geq 3$).

by sublimation. In principle distinct pore structures and sizes can be achieved by using different freezing regimes [32–34]. Therefore, we have compared the effect of three different freezing regimes on the pores of the omentum scaffolds. The 1% hydrogels were molded in three different plates and frozen in different manners: snap frozen in liquid nitrogen ($-196\text{ }^\circ\text{C}$), in a $-20\text{ }^\circ\text{C}$ freezer, or in a $-20\text{ }^\circ\text{C}$ freezer inside an isopropanol bath to further slowdown the freezing process. SEM images of longitudinal and horizontal cross sections revealed a distinct internal morphology of the scaffolds (Fig. 3). While freezing with $-20\text{ }^\circ\text{C}$ resulted in large, rounded, interconnected open pores, the snap freezing induced amorphous, nonhomogeneous fibrous structure (Fig. 3A). Further quantification of the pore area (Fig. 3B) revealed that the average pore size of the slow-frozen ($-20\text{ }^\circ\text{C}$ in isopropanol) scaffolds ($0.028 \pm 0.003\text{ mm}^2$) was approximately 3 fold larger than the average pore size of the $-20\text{ }^\circ\text{C}$ frozen scaffolds ($0.01 \pm 0.001\text{ mm}^2$), and >15 fold larger than the average pore size of those that were snap frozen ($0.0017 \pm 0.001\text{ mm}^2$). These results indicate that the slower the freezing process is, the larger the pores, due to the larger ice crystals that are gradually formed in the hydrogel. As the cells in the hematopoietic niche reside in large clusters in rounded pores, the scaffolds fabricated by the slow freezing regimen are the most suitable for hematopoietic cell culture.

We next sought to determine the effect of ECM concentration on porosity and stability of the scaffolds. Different quantities of decellularized omentum powder were digested in pepsin solution in order to obtain different hydrogel concentrations (0.5%, 1% or 1.5% w/v). The hydrogels were physically cross-linked, frozen in isopropanol bath at $-20\text{ }^\circ\text{C}$ and lyophilized. As can be seen in Fig. 4A, although the lyophilized scaffolds had approximately the same volume, after rehydration, the 0.5% scaffold collapsed and lost its original shape.

We speculated that ECM concentration may also affect pore size. Therefore, the scaffolds were imaged by SEM and the internal structure was assessed (Fig. 4B and C). As expected, higher concentration of the ECM components resulted in smaller pores. The measured pore areas of the 1.5%, 1% and 0.5% scaffolds were $0.0167 \pm 0.002\text{ mm}^2$, $0.0251 \pm 0.003\text{ mm}^2$ and $0.03 \pm 0.001\text{ mm}^2$, respectively. Differences were also detected in the total porosity of the scaffolds (defined in Section 2, Fig. 4D). The 1.5% scaffold had 0.49 ± 0.01 porosity, which was significantly ($p < 0.0001$) lower than the 1% and the 0.5% scaffolds porosity (0.66 ± 0.01 and 0.78 ± 0.01 respectively). Due to the loss of volume of the 0.5% scaffold after rehydration (Fig. 4A), it can be deduced that the porous structure was not preserved.

As hematopoietic stem cell expansion takes place over a period of several weeks, it is essential to assess the stability of the scaffolds over time. As shown, after 20 days of incubation in PBS at $37\text{ }^\circ\text{C}$, only a slight

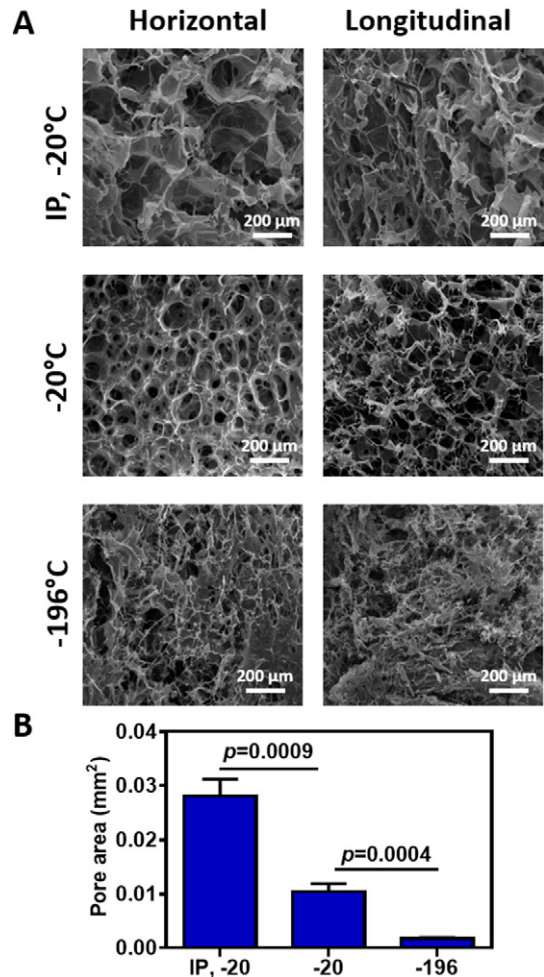


Fig. 3. Different freezing regimes effect on pore size. A. Representative SEM images of the horizontal and longitudinal cuts of the omentum scaffolds that were formed by the different freezing regimes. B. Mean pore area (in mm²) of the different scaffolds, measured from the horizontal images. ($n = 5$ scaffolds in each group).

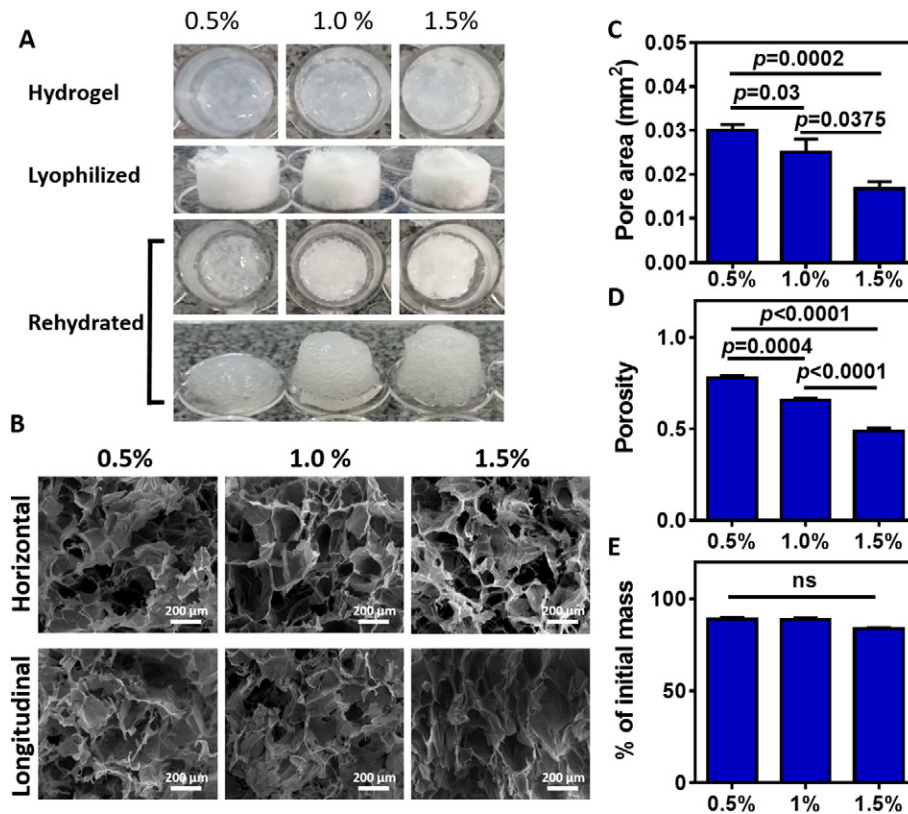


Fig. 4. Effect of ECM concentration on scaffolds' properties. A. View on the different gels formation and macro-structure before and after rehydration. B. Representative SEM images of the horizontal and longitudinal cuts of the omentum scaffolds in different concentrations. C. Mean pore area (in mm²) of the different scaffolds, measured from the horizontal images. (n = 5 images). D. Mean porosity of the different scaffolds, calculated as the relation between the void volume and the initial volume before lyophilizing (n = 4). E. Degradation of the scaffolds after 20 days in PBS at 37 °C (n = 4).

degradation of the scaffolds of all concentrations was observed, as judged by the preservation of the original mass (Fig. 4E). As hematopoietic cells may be sensitive to changes in the mechanical properties of their substrate [35,36], the low degradation rate ensures that the cells are exposed to a stable microenvironment.

After considering all the discussed aspects of the different scaffolds, we have decided to work with the slow-frozen 1% scaffolds, in order to obtain a stable structure with large pores.

Within the body, the s-GAGs electrostatically bind growth factors, cytokine and chemokines and release them into the cellular microenvironment. Therefore, we next sought to evaluate the ability of the s-GAGs within the pores of the scaffolds to bind factors that may be useful in an engineered hematopoietic niche. To determine the scaffolds' potential to serve as a depot for growth factors, we measured their loading capacity and the release profile of relevant factors. SCF, Flt3-L and VEGF were loaded in different concentrations (50, 100, 200 and 400 ng/scaffold) on 1%, 0.1 ml scaffolds in 96-well low-binding plates. Post incubation of 2 h, the scaffolds were washed and digested. The amount of loaded factors that were extracted from the scaffolds was determined using ELISA. As shown in Fig. 5A, the scaffolds were able to bind the 50 ng factors in the most efficient way. Moreover, Flt3-L was able to efficiently bind the scaffolds at all concentrations, while the 100 ng of SCF and VEGF could only bind in a partially manner. The limited ability of the scaffold to bind the factors may indicate that the s-GAGs were already occupied and the factors reached saturation.

Next, we sought to evaluate the dissociation of the factors from the scaffolds and their release into the cellular microenvironment. The release profile of the different factors (50 ng) was monitored after loading the scaffolds. As shown in Fig. 5B–D, after 10 days of incubation, the factors were slowly released into the medium (20.84 ± 1.74% of SCF, 11.84 ± 0.2% of VEGF, and 23.63 ± 0.56% of Flt3-L). The low amount

of the released factors may indicate that the rest of the factors were bound to the pore walls of the scaffolds, which may have protected them from degradation. Moreover, as many factors can be presented to cells and affect them without complete release, their attachment to the pore walls may be another advantage of the system. Overall, these results suggest that the scaffolds are capable of capturing and releasing important factors that are abundant in the natural hematopoietic stem cells environment [6,37,38].

Finally, we sought to evaluate the ability of the ECM-based scaffolds to support hematopoietic cells. Therefore, as a proof-of-concept we have chosen to use the EML cell line as a simplified model for hematopoietic stem cells. EML cells are immortalized cells derived from murine bone marrow [39]. Given different factors, these cells are capable of differentiation or self-renewal *in vitro* [40]. In order to proliferate, these cells require a medium supplemented with at least 200 ng/ml SCF. When given lower SCF concentrations, the proliferation rate is lower and cell death rate is higher, resulting in low cell viability after 72 h (Fig. 6A). SCF is a heparin-binding protein. In the bound state, the heparin binding factors are protected from proteolysis and are often going through conformational changes that induce receptor-factor binding. The GAGs may also mediate clustering of the growth factor to the cell surface, thus enhancing the factors activity [41]. Therefore, we hypothesized that when bound to the scaffold, lower concentrations of SCF are required for sufficient self-renewal. As shown in Fig. 6B, the fold expansion of EML on the 50 ng/ml and 200 ng/ml SCF-loaded scaffold (6.48 ± 0.55 and 11.26 ± 2 respectively) was higher than the fold expansion of the EML cells in suspension (2.746 ± 0.1405 and 8.425 ± 0.09761, respectively). When no SCF was added, the fold expansion of EML on the scaffold was 1.088 ± 0.17, indicating that although the cells did not proliferate for 3 days, they remained viable, as appose to the cells grown in suspension (0.23 ± 0.06).

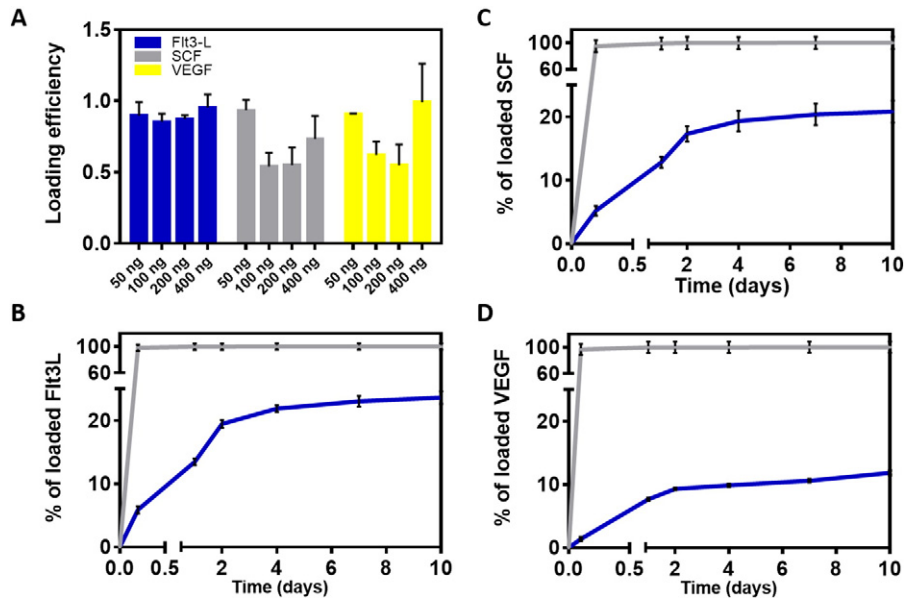


Fig. 5. Loading efficiency and release profile. A. Loading efficiency of Flt3-L, SCF and VEGF in different concentrations, normalized to the initial loaded amount (n = 3). B–D. Release profiles of 50 ng of Flt3-L, SCF and VEGF from the scaffolds (n = 3).

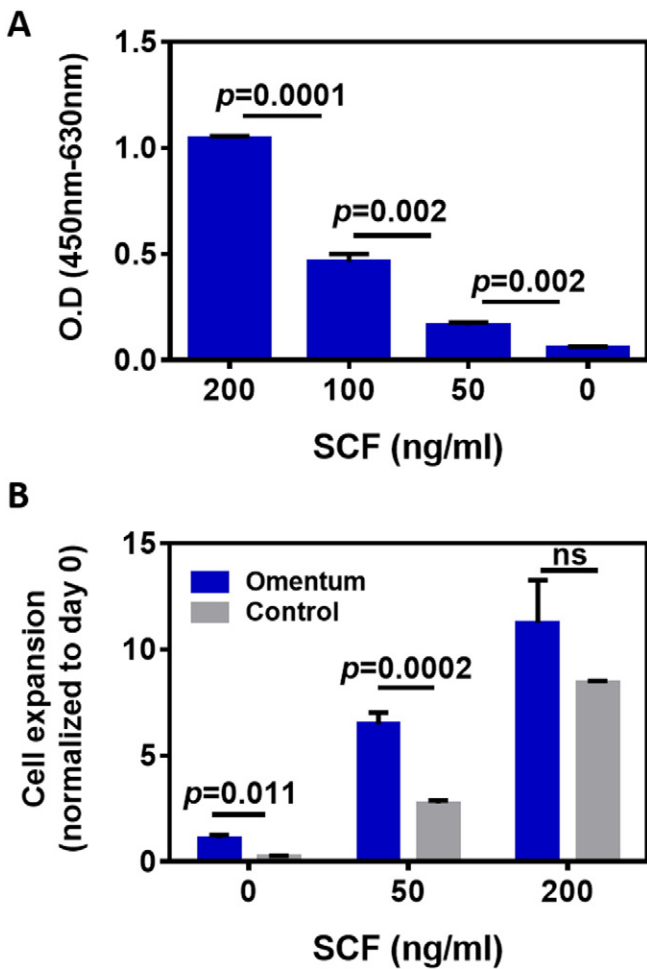


Fig. 6. EML proliferation. A. Cell viability after 72 h incubation with different concentrations of SCF (0–200 ng/ml). Results are represented as the mean delta between the optical densities (O.D) at 450 nm and at 630 nm (n = 3). B. EML cell growth on SCF-loaded scaffolds (final concentrations of 0, 50 or 200 ng/ml) or in suspension. The viability was measured by XTT at day 0 and after 72 h. Results are represented as the mean relation between the O.D at day 3 and on day 0 (n ≥ 3).

These results primly indicate that our porous omentum-based scaffold is a biocompatible environment for hematopoietic cell growth. Secondly, the high fold expansion of the EML cells with only 25% of the recommended SCF concentration implies that the SCF activity is indeed increased due to the binding effect.

4. Conclusions

An efficient *ex vivo* expansion of hematopoietic stem cells has not yet been accomplished. In order to proliferate, HSCs require special topography and biochemical components. Here, we described the development of a stable biocompatible macroporous scaffold that is composed of the omental decellularized ECM. We have investigated the biochemical content of the scaffold, and further optimized the scaffold's porous structure by adjusting the material concentration and freezing regime before freeze-drying. Our findings show that the omentum sponges are composed mainly of collagens and GAGs. We have also shown that soluble factors could strongly bind to the scaffolds and be slowly released from them, suggesting s-GAGs-protein interaction, similar to the one occurring *in vivo*. We have further shown the potential of the factors-loaded scaffold to serve as a platform for cell proliferation, using the SCF-dependent EML cells as a model. The bound SCF was functional and enhanced better EML proliferation, even in lower concentrations. However, to prove the real potential of this 3D platform for *ex-vivo* expansion of HSCs, more experiments should be carried with primary hematopoietic stem cells.

Acknowledgment

TD acknowledges partial support from the Israel Science Foundation Individual Grant 700/13. The work is part of the doctoral thesis of NST.

References

- [1] J.A. Schuster, M.R. Stupnikov, G. Ma, W. Liao, R. Lai, Y. Ma, J.R. Aguila, Expansion of hematopoietic stem cells for transplantation: current perspectives, *Exp. Hematol. Oncol.* 1 (2012) 12.
- [2] R. Sugimura, Bioengineering hematopoietic stem cell niche toward regenerative medicine, *Adv. Drug Deliv. Rev.* 99 (2016) 212–220.
- [3] K. Chotinantakul, W. Leeanansaksiri, Hematopoietic stem cell development, niches, and signaling pathways, *Bone Marrow Res.* 2012 (2012) 270425.
- [4] D.S. Krause, Regulation of hematopoietic stem cell fate, *Oncogene* 21 (2002) 3262–3269.

- [5] W. Leeansaksiri, C. Dechsukhum, Regulation of stem cell fate in hematopoietic development, *J. Med. Assoc. Thai.* 89 (2006) 1788–1797.
- [6] A. Mendelson, P.S. Frenette, Hematopoietic stem cell niche maintenance during homeostasis and regeneration, *Nat. Med.* 20 (2014) 833–846.
- [7] S.F. Badylak, D.O. Freytes, T.W. Gilbert, Extracellular matrix as a biological scaffold material: structure and function, *Acta Biomater.* 5 (2009) 1–13.
- [8] T. Hoshiba, H. Lu, N. Kawazoe, G. Chen, Decellularized matrices for tissue engineering, *Expert Opin. Biol. Ther.* 10 (2010) 1717–1728.
- [9] R. Langer, J.P. Vacanti, Tissue engineering, *Science* 260 (1993) 920–926.
- [10] R. Manabe, K. Tsutsui, T. Yamada, M. Kimura, I. Nakano, C. Shimono, N. Sanzen, Y. Furutani, T. Fukuda, Y. Oguri, K. Shimamoto, D. Kiyozumi, Y. Sato, Y. Sado, H. Senoo, S. Yamashina, S. Fukuda, J. Kawai, N. Sugiura, K. Kimata, Y. Hayashizaki, K. Sekiguchi, Transcriptome-based systematic identification of extracellular matrix proteins, *Proc. Natl. Acad. Sci. U. S. A.* 105 (2008) 12849–12854.
- [11] S.F. Badylak, The extracellular matrix as a biologic scaffold material, *Biomaterials* 28 (2007) 3587–3593.
- [12] T.W. Gilbert, T.L. Sellaro, S.F. Badylak, Decellularization of tissues and organs, *Biomaterials* 27 (2006) 3675–3683.
- [13] H.C. Ott, T.S. Matthiesen, S.K. Goh, L.D. Black, S.M. Kren, T.I. Netoff, D.A. Taylor, Perfusion-decellularized matrix: using nature's platform to engineer a bioartificial heart, *Nat. Med.* 14 (2008) 213–221.
- [14] L.E. Flynn, The use of decellularized adipose tissue to provide an inductive microenvironment for the adipogenic differentiation of human adipose-derived stem cells, *Biomaterials* 31 (2010) 4715–4724.
- [15] S.E. Dahms, H.J. Piechota, R. Dahiya, T.F. Lue, E.A. Tanagho, Composition and biomechanical properties of the bladder acellular matrix graft: comparative analysis in rat, pig and human, *Br. J. Urol.* 82 (1998) 411–419.
- [16] K. Schenke-Layland, O. Vasilevski, F. Opitz, K. Konig, I. Riemann, K.J. Halhuber, T. Wahlers, U.A. Stock, Impact of decellularization of xenogeneic tissue on extracellular matrix integrity for tissue engineering of heart valves, *J. Struct. Biol.* 143 (2003) 201–208.
- [17] J.E. Valentin, J.S. Badylak, G.P. McCabe, S.F. Badylak, Extracellular matrix bioscaffolds for orthopaedic applications. A comparative histologic study, *J. Bone Joint Surg. Am.* 88 (2006) 2673–2686.
- [18] D. Collins, A.M. Hogan, D. O'Shea, D.C. Winter, The omentum: anatomical, metabolic, and surgical aspects, *J. Gastrointest. Surg.* 13 (2009) 1138–1146.
- [19] S. Huyghe, H. de Rooster, M. Doom, W. Van den Broeck, The microscopic structure of the omentum in healthy dogs: the mystery unravelled, *Anat. Histol. Embryol.* 45 (2016) 209–218.
- [20] S. Shichijo, H. Masuda, Further studies on glycosaminoglycans in the human greater omentum, *Int. J. Biochem.* 11 (1980) 501–506.
- [21] R.S. Patel, A.A. Makitie, D.P. Goldstein, P.J. Gullane, D. Brown, J. Irish, R.W. Gilbert, Morbidity and functional outcomes following gastro-omental free flap reconstruction of circumferential pharyngeal defects, *Head Neck* 31 (2009) 655–663.
- [22] E.L. Shelton, S.D. Poole, J. Reese, D.M. Bader, Omental grafting: a cell-based therapy for blood vessel repair, *J. Tissue Eng. Regen. Med.* 7 (2013) 421–433.
- [23] N. Soffer-Tsur, M. Shevach, A. Shapira, D. Peer, T. Dvir, Optimizing the biofabrication process of omentum-based scaffolds for engineering autologous tissues, *Biofabrication* 6 (2014) 035023.
- [24] U. Lindahl, M. Hook, Glycosaminoglycans and their binding to biological macromolecules, *Annu. Rev. Biochem.* 47 (1978) 385–417.
- [25] M. Shevach, R. Zax, A. Abrahamov, S. Fleischer, A. Shapira, T. Dvir, Omentum ECM-based hydrogel as a platform for cardiac cell delivery, *Biomed. Mater.* 10 (2015) 034106.
- [26] S.R. Meyer, J. Nagendran, L.S. Desai, G.R. Rayat, T.A. Churchill, C.C. Anderson, R.V. Rajotte, J.R. Lakey, D.B. Ross, Decellularization reduces the immune response to aortic valve allografts in the rat, *J. Thorac. Cardiovasc. Surg.* 130 (2005) 469–476.
- [27] P.M. Crapo, T.W. Gilbert, S.F. Badylak, An overview of tissue and whole organ decellularization processes, *Biomaterials* 32 (2011) 3233–3243.
- [28] J.D. Esko, R.J. Linhardt, Proteins that bind sulfated glycosaminoglycans, in: V. A. C. RD, E. JD (Eds.), *Essentials of Glycobiology*, Cold Spring Harbor Laboratory Press, Cold Spring Harbor (NY), 2009.
- [29] A.K. Powell, E.A. Yates, D.G. Fernig, J.E. Turnbull, Interactions of heparin/heparan sulfate with proteins: appraisal of structural factors and experimental approaches, *Glycobiology* 14 (2004) 17R–30R.
- [30] Q.L. Loh, C. Choong, Three-dimensional scaffolds for tissue engineering applications: role of porosity and pore size, *Tissue Eng. B Rev.* 19 (2013) 485–502.
- [31] R. Gauvin, Y.C. Chen, J.W. Lee, P. Soman, P. Zorlutuna, J.W. Nichol, H. Bae, S. Chen, A. Khademhosseini, Microfabrication of complex porous tissue engineering scaffolds using 3D projection stereolithography, *Biomaterials* 33 (2012) 3824–3834.
- [32] H.W. Kang, Y. Tabata, Y. Ikada, Fabrication of porous gelatin scaffolds for tissue engineering, *Biomaterials* 20 (1999) 1339–1344.
- [33] F.J. O'Brien, B.A. Harley, I.V. Yannas, L. Gibson, Influence of freezing rate on pore structure in freeze-dried collagen-GAG scaffolds, *Biomaterials* 25 (2004) 1077–1086.
- [34] S. Zmora, R. Glicklis, S. Cohen, Tailoring the pore architecture in 3-D alginate scaffolds by controlling the freezing regime during fabrication, *Biomaterials* 23 (2002) 4087–4094.
- [35] F. Gattazzo, A. Urciuolo, P. Bonaldo, Extracellular matrix: a dynamic microenvironment for stem cell niche, *Biochim. Biophys. Acta* 1840 (2014) 2506–2519.
- [36] K. Song, L. Li, Y. Wang, T. Liu, Hematopoietic stem cells: multiparameter regulation, *Hum. Cell* 29 (2016) 53–57.
- [37] P.E. Boulais, P.S. Frenette, Making sense of hematopoietic stem cell niches, *Blood* 125 (2015) 2621–2629.
- [38] K. Kirito, N. Fox, N. Komatsu, K. Kaushansky, Thrombopoietin enhances expression of vascular endothelial growth factor (VEGF) in primitive hematopoietic cells through induction of HIF-1 α , *Blood* 105 (2005) 4258–4263.
- [39] S. Tsai, S. Bartelmez, E. Sitnicka, S. Collins, Lymphohematopoietic progenitors immortalized by a retroviral vector harboring a dominant-negative retinoic acid receptor can recapitulate lymphoid, myeloid, and erythroid development, *Genes Dev.* 8 (1994) 2831–2841.
- [40] S. Zong, S. Deng, K. Chen, J.Q. Wu, Identification of key factors regulating self-renewal and differentiation in EML hematopoietic precursor cells by RNA-sequencing analysis, *J. Vis. Exp.* (2014) e52104.
- [41] A. Lowman, A. Dillow, Biomimetic materials and design: biointerfacial strategies, *Tissue Engineering and Targeted Drug Delivery*, 2002.